

Temperature dependence of carrier relaxation in semiconductor doped glasses

G. Beadie

Department of Physics, Brown University, Providence, Rhode Island 02912

E. Sauvain

Division of Engineering, Brown University, Providence, Rhode Island 02912

A. S. L. Gomes

Departamento de Fisica, Universidade Federal de Pernambuco, Recife, Pernambuco, Brazil

N. M. Lawandy

Division of Engineering and Department of Physics, Brown University, Providence, Rhode Island 02912

(Received 13 June 1994)

Two-color picosecond pump-probe measurements in semiconductor nanocrystallite doped glasses reveal nonexponential decay of photoexcited carriers. The dependence of the decay on nanocrystallite size, pump intensity, temperature, and probe wavelength are examined and discussed within the framework of continuous-time random-walk models for transport of carriers among localized trap sites. This analysis suggests that carrier transport in lower dimensions is involved in the relaxation of these nanoscale systems.

I. INTRODUCTION

Since the discovery of Jain and Lind¹ of fast nonlinear optical response in semiconductor-doped glasses, semiconductor nanocrystalline systems have been studied extensively. An understanding of the excitonic energy spectrum of these quantum-confined structures started first with Éfros and Éfros.² Using a modified effective-mass approach, they were able to predict qualitatively the dependence of exciton energies on particle size. This first approximation, however, did not include the effects of finite potential barriers at the surface of the crystallite, the dielectric contrast at the interface between the crystallite and the host medium, the effects of defects either in the crystallite or on its surface, or the effect of a nonspherical particle. Later treatments became successively more sophisticated, allowing for better agreement with experiment, but it became clear that the nature of the surface interfacial properties hindered quantitative predictions of experimentally observed energy levels.

Determining the nature of the time response of these materials has been difficult. Groups have observed time-varying, nonexponential phenomena in every regime from femtoseconds to hours, depending on the type of excitation implemented. Part of the problem was resolved with the empirical observation of Roussignol *et al.*³ that these materials change their optical properties upon laser irradiation. This observation served to make experiments more consistent with one another, but the underlying physics of this so-called photodarkening effect is still a debated topic. On the other hand, what has become clear is that surface states play an important role in the relaxation dynamics of these materials. Experiments performed on crystallites suspended in solution have shown that

both the luminescence intensity and the luminescence as a function of time depend upon the presence of surface-binding chemical species present in the solvent.^{4,5} Woggon *et al.*⁶ also noticed a sharp difference in the response of thin semiconductor-doped glass samples which were exposed to hot H₂ gas. They proposed that the hydrogen diffused into the glass and changed its behavior by binding to the crystalline surfaces. These experiments along with later studies⁷⁻¹³ have shown unambiguously the importance of surface effects in these materials.

Because of the clear presence of surface-dependent effects and because of the nature of the decays observed in the majority of experiments, models of the relaxation behavior are often based upon a multilevel deexcitation scheme involving linear transition rates between bulk and surface states. These models consistently predict multiexponential behavior to account for the nonexponential decays.¹⁴⁻¹⁷ Nonlinear models involving bimolecular or Auger terms are also considered to predict the decays of experiments designed to produce many carriers per crystallite, a regime in which these nonlinear effects become important.¹⁸

A different approach to fit data empirically was taken by O'Neil, Marohn, and McLendon.⁶ Unable to fit their data to multiexponentials satisfactorily, despite their very low-intensity excitation source, they included a stretched exponential term $\exp\{-(t/\tau)^\beta\}$, to their fitting function, a term related to distributed kinetics models. As motivation for introducing the term, they cite James and Ware,¹⁹ who show that multiexponential fits to decay data can be greatly misleading. They argue that a more appropriate term is one predicted by distributed kinetics, as is the stretched exponential, but they make it clear that they assign no physical meaning to their overall

fitting function.

In this work we further examine the relaxation phenomena in a commercially available borosilicate glass matrix embedded with nanocrystallites of $\text{CdS}_x\text{Se}_{1-x}$. In Sec. II we give a description of the samples that were investigated and the apparatus used to study them. In Sec. III we outline our method of interpreting data using a stretched exponential, and present temperature-dependent results based on this analysis. Section IV is devoted to a discussion of the physical models which we use to interpret our results, and a justification for the picture we adopt: that of excited carriers quickly localizing to surface states on the crystallites, and recombining on recombination centers reached via continuous-time random walks.

II. EXPERIMENT

The sample used for this study was a commercially available, long-pass filter glass RG610 from Schott Glass

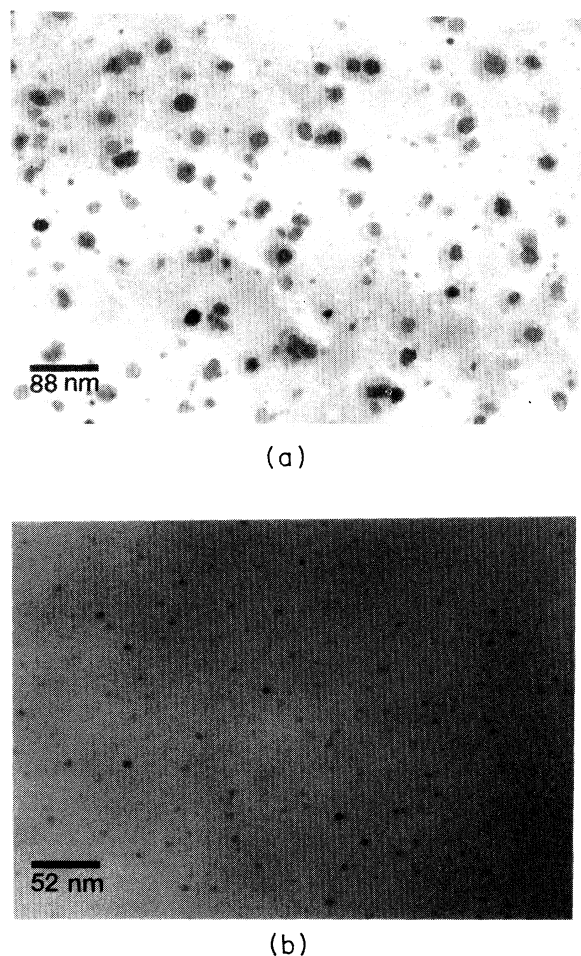


FIG. 1. Bright field transmission electron micrograph of glasses *A* and *B* in (a) and (b), respectively. The samples were mechanically thinned and dimpled, then ion milled and carbon coated. The darker spherical dots are the nanocrystallites. The nanocrystallites in glass *A* are observed to possess an elongated and faceted shape.

Inc. This composite system is comprised of a colloidal suspension of $\sim 0.1\%$ by volume fraction $\text{CdS}_x\text{Se}_{1-x}$ nanocrystals in a borosilicate glass matrix. A transmission electron microscopy (TEM) micrograph of this material [see Fig. 1(b)] shows that the glass contains roughly spherical nanocrystallites with an average diameter of 6.5 ± 4 nm. Experiments were also performed on a glass sample that was heat treated at 645°C for 48 h. The result of this treatment was a growth of the nanocrystals to an average diameter of 18 ± 9 nm [see Fig. 1(a)], thereby increasing their area by a factor of 7.6 and their volume by a factor of 21. The volume-to-surface ratio increased from ~ 2 in the small crystallites to ~ 6 in the larger ones. In addition, the larger crystallites acquired some of the elongated and faceted shape characteristics of large crystallites.²⁰ The heat-treated glass and virgin glass will be designated glass *A* and glass *B*, respectively.

Linear absorption and luminescence data for each glass are given in Fig. 2. The absorption spectra, taken from $250\text{-}\mu\text{m}$ -thick samples, exhibit bumps which are characteristic of electron-hole-confined states, and, as expected²¹ are more prominent in the small crystallite sample. Also shown are least-squares fits of the data to $\alpha = A\sqrt{h\nu - E_g}$, the calculated absorption spectrum of a direct gap, parabolic band semiconductor.²² The absorption tails which extend beyond the parabolic absorption bands are most likely due to distributions of localized trap states rather than to size confinement effects related

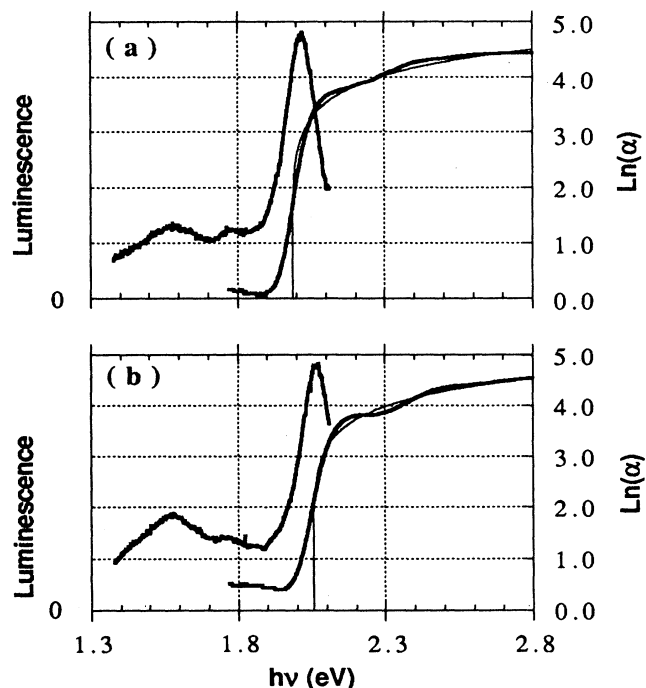


FIG. 2. Linear absorption and luminescence curves for glasses *A* and *B* in (a) and (b), respectively. Also shown as the thinner curves are least-squares fits to the absorption data of the calculated absorption spectrum, $\alpha = A\sqrt{h\nu - E_g}$, of a direct gap, parabolic band semiconductor. α is given in cm^{-1} before the logarithm is taken. The luminescence peak of (b) is a factor of $\frac{15}{8}$ larger than that of (a).

III. RESULTS AND DISCUSSION

A. Stretched exponential fits

A representative pump-probe decay curve is shown in Fig. 4, along with least-squared fits to two common fitting functions: the single exponential and the double exponential, the latter arising from linear relaxation models.^{14–17} The data for the change in transmission ΔT are better described by a double exponential $A \exp\{-at\} + B \exp\{-bt\}$, but the fit clearly oscillates about the smooth decay of the data. If we truncate our data to include only $1-1\frac{1}{2}$ decades of time, the discrepancy is observed to become much smaller; it is only by utilizing the full time range of this experiment that the qualitative weakness of the double exponential fit becomes apparent. On the other hand, as shown in Fig. 5, the stretched exponential fit to the data, $A \exp\{-(t/\tau)^\beta\}$, smoothly follows the decay. The major area of discrepancy occurs within the first 30 ps of the decay. As we shall see below, the models that predict stretched exponential decay predict different forms in the short-time limit of the decay. For this reason, and to account for pulse-shaping effects, we allow the overall multiplicative constant A to vary when we perform our least-squared fits despite having normalized the maximum of the decay at time “zero” to one.

Similarly, it must be noted that in glass *B* a slow, time-varying absorptive recovery was observed at low temperatures which caused some of the data curves to extend below the dc offset level achieved before the pump pulse arrived. An example curve is shown in Fig. 6. This behavior is indicative of an effect that is slow compared to the 4-ns time scale of our experiment but comparable to the 14-ns period of the mode-locked laser pulses. In order to extract fitting parameters from such curves, we fit the data to a stretched exponential equipped with an artificial offset, C :

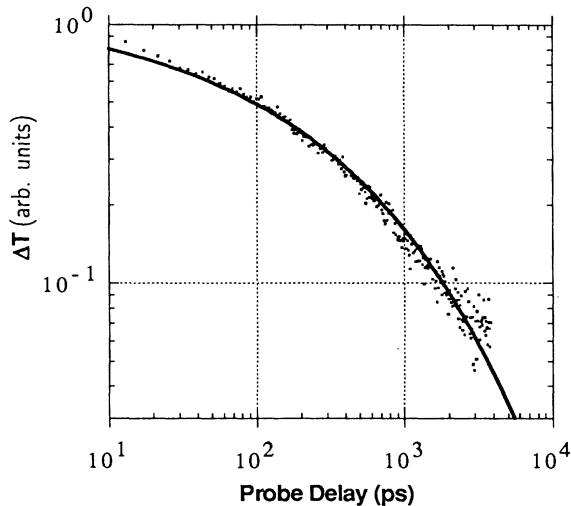


FIG. 5. Shown here are the same data as depicted in Fig. 4, along with the best stretched exponential fit $A \exp\{-(t/\tau)^\beta\}$ to the decay.

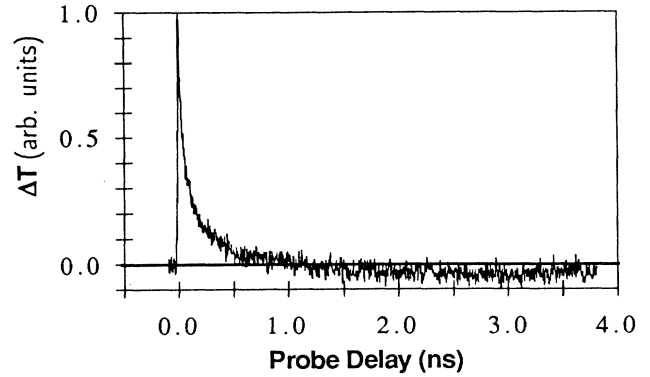


FIG. 6. Glass *B* data exhibiting a slow absorptive recovery. The data before the peak represent the recovery obtained between excitation pulses (13 ns).

$$\Delta T = A \left\{ \frac{\exp[-(t/\tau)^\beta] - C}{1 - C} \right\}, \quad (1)$$

and allowed C to vary along with A , τ , and β . Four different sets of data from this sample, unaffected by the absorptive recovery, were fitted with both this function and the regular stretched exponential fit. In each case the returned values of τ and β differed by less than our experimental uncertainty.

B. Intensity and exposure sensitivity

The behavior of the dynamics as a function of both intensity and laser exposure was explored in detail at room temperature. Two different intensity measurements were performed. In one experiment the modulation of the pump beam was kept the same while the overall average power was varied. In another experiment the average power was held constant while the duty cycle of the modulation was modified. In the first case, primarily the effects of sample heating were probed, while in the second case the dependence on initial carrier concentration was probed. In each case only a weak dependence of the decays on pump power was observed from 0.2 to 1.2 kW/cm². There are two primary conclusions that we may draw from these experiments: (1) Auger recombination, observed in other situations involving higher pump intensities, is negligible in our system; and (2) β is independent of power over our experimental range of pump powers.

Most importantly, however, the dependence of the dynamics as a function of laser exposure was also studied. This effect had to be carefully scrutinized, since it is well known that the response time is a function of photodarkening. To examine this effect in our samples, we exposed a virgin spot of glass *A* to 50-mW average pump power focused down to a 60- μ m-diameter spot, and obtained relaxation data at various times during the exposure. A plot of the τ and β parameters as a function of exposure time is given in Fig. 7. It is clear here that β is independent of pump exposure. This is a crucial result, validating

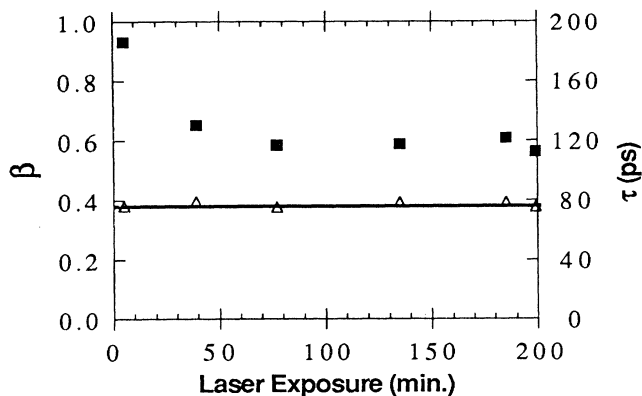


FIG. 7. Plot of fitting parameters vs laser exposure time for a virgin spot of glass *A*. Filled squares represent τ , open triangles represent β .

all our data on β from the point of view of photodarkening effects.

C. Temperature dependencies

Changing the temperature affects many of the optical properties of these materials. As in a bulk semiconductor, for example, changing the temperature changes the band-gap energy. Temperature-dependent luminescence measurements undertaken on glass *B* indicate that between room temperature and 600 K the change in band gap with temperature is linear with a slope of -7.2×10^{-4} eV/K. This is in very good agreement with Borrelli *et al.*,²³ from whose data on $\text{CdS}_x\text{Se}_{1-x}$ doped glasses can be extracted a value of -7.3×10^{-4} eV/K, quite different from the value of -4×10^{-4} eV/K quoted for bulk CdSe.²⁴ Thus, by heating the sample yet keeping the probe wavelength fixed, one can shift the band edge below the energy of the probe, in effect changing the states probed by the probe beam. To investigate the dependence of the relaxation on this shift, we first heated glass *B* to a temperature at which the luminescence peak was centered on the dye response curve, and then tuned the probe laser above and below the luminescence peak to see whether there was a change in the dynamics. (see Fig. 8). Clearly, there is no dependence of the relaxation on the position of the probe beam within the first luminescence peak.

It may be noted, however, that cooling from room temperature down to 4 K with an extrapolated -7.2×10^{-4} eV/K band-gap variation results in a band-gap increase of over 200 meV. Assuming that the whole energy structure shifts with the change of band gap, this would imply that at 4 K the experiment probes states that are 200 meV below those investigated at room temperature. At first glance, this appears to be particularly disturbing, since room-temperature luminescence curves (Fig. 2) display marked trap peaks at these energies. We claim, however, that since luminescence relaxation involving these trap states have been shown to exhibit μs decay times, they should not affect any studies carried out on a picosecond time scale.¹⁵ We argue that our transient sig-

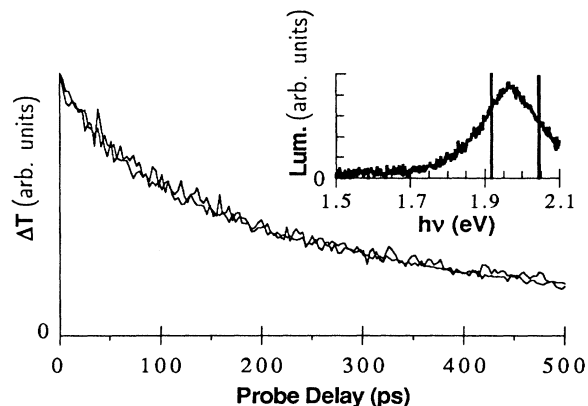


FIG. 8. Glass *B* decay data from two sides of a high-temperature ($T=452$ K) luminescence peak. The inset shows the corresponding high-temperature luminescence, and the vertical lines indicate the two probe energies.

nals are due to the same states that form the primary luminescence peak, but are probed out in the tail of their overall distribution. This is in qualitative agreement with the smaller signal intensities we observe at colder temperatures: small enough that in glass *B* we could not obtain reliable data below 50 K for the pump-probe measurements.

The temperature-dependent decay data are shown in Fig. 9. Both glasses are observed to have two distinct temperature regimes with respect to β . At lower temperatures, β remains nearly constant, while at higher temperatures β increases linearly with increasing T . It was also observed that from room temperature down to 4 K, τ went up from 50 to 160 ps for glass *A* and from 50 ps to over 260 ps for glass *B*.

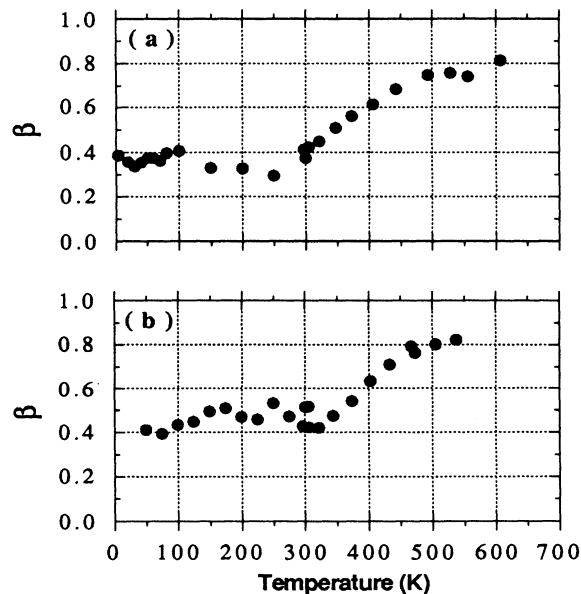


FIG. 9. β vs temperature for glasses *A* and *B* in (a) and (b), respectively.

IV. ANALYSIS OF THE DECAY DATA

We choose to analyze our data using a stretched exponential decay fit. Stretched exponentials are characteristic of systems which exhibit broad distributions of event times. Since this is a property independent of specific microscopic details, stretched exponential behavior has been observed in a wide variety of experiments, such as those involving polymer relaxation,²⁵ dielectric response of glassy systems,²⁶ carrier recombination in *a*-Si,²⁷ and remnant magnetization in spin glasses.²⁸ A general feature of these systems is that they all display disorder of some type. It is the disorder which creates the distribution of event times that gives rise to this nonexponential behavior.

Stretched exponential behavior associated with sequential-parallel processes (carriers moving then recombining) is predicted in the literature by several versions of random-walk models. We will analyze our data using a pseudounimolecular, continuous-time random-walk "trapping model" which contains the salient features required to explain the relaxation process.²⁹ In this model, a survival probability is calculated for one carrier moving randomly on a geometrical structure characterized by its dimension d and a density p of some fixed recombination centers. With the assumption of independent carriers, the survival probability of a population of carriers is given by the same function.

An element of any continuous-time random walk is $\psi(t)$, the probability distribution that a carrier sitting on a site will move to a next site after a time t . The form of $\psi(t)$ depends upon the model used to describe transport between sites, and determines the survival probability of the carrier as a function of time, $\Phi(t)$. If the first moment τ_0 of $\psi(t)$ is finite, one expects a long-time asymptotic form of²⁹

$$\Phi(t) \propto \exp \left\{ -Cp^{2/(d+2)} \left(\frac{t}{\tau_0} \right)^{d/(d+2)} \right\}, \quad (2)$$

where C is a numerical constant assumed to be of the order of unity, and β is temperature independent and equal to $d/(d+2)$. Since both hopping transport and tunneling between localized states may be characterized by a mean time, one expects decays governed by either of these types of transport to be characterized by Eq. (2) in the long-time limit. It must be noted that though Eq. (2) has been rigorously proven for this model, the convergence of computer simulations cited in Ref. 29 is very slow for $d > 1$, becoming unobservable at $d \geq 3$.

If τ_0 is not finite, we expect a different behavior for $\Phi(t)$. In the multiple trapping model of transport, for example, carriers are thermally ejected from and retrapped in an exponential distribution of trap states below a mobility edge. τ_0 for this model diverges, since $\psi(t)$ is calculated to exhibit a long-time algebraic tail. In this case, one expects the medium-time limit of the decay (not well defined; see Ref. 29 of the derivation and Refs. 30 and 31 for applications) to be a stretched exponential with a temperature-dependent $\beta = (T/T_0)(d/2)$, where T_0 is the characteristic temperature of the distribution of trap states and $d < 2$, or $\beta = T/T_0$ for $d > 2$.³² This model

holds for $T < T_0$; above $\sim T_0$, diffusion starts to govern the transport and β is expected to saturate near 1.

If these models are to be consistent with the rapid (≤ 10 ps) transfer of photogenerated carriers to surface states, as suggested by previous studies,³³⁻³⁵ we expect the observed relaxation dynamics (1) to be dependent on a low-dimensionality random-walk process of some kind, and (2) to be intensity independent for intensities not too high. The latter was observed, as mentioned in Sec. III B. In order to explore the former possibility, we measured the temperature dependence of the fit parameter β over a range of temperatures from 4 to 600 K. The results shown in Fig. 9 show that for both samples β has a temperature-independent region from 4 to 250 K, and then behaves in an essentially linear fashion from 300 to 450 K. The linear behavior at higher temperatures, $\beta \sim T/T^*$, is predicted by the multiple-trapping model, where $T^* = 2T_0/d$ for $d < 2$ and $T^* = T_0$ for $d > 2$. T_0 can be estimated independently from the absorption tails in Fig. 2, as mentioned in Sec. II, as well as by the temperature at which β begins to saturate. T^* , as measured from the slopes of the two lines, is 510 ± 50 K for glass *A* and 500 ± 30 K for glass *B*. Using these results we can extract the dimension d on which the multiple-trapping transport takes place. At high temperatures, the data reveal that $d = 1.8 \pm 0.3$ and 2.0 ± 0.2 for glasses *A* and *B*, respectively, consistent with multiple trapping taking place on the surface of the crystallites. Note that because of the near equivalence between T^* and T_0 in glass *B*, we cannot formally distinguish between $d = 2$ and $d > 2$. The data are consistent with $d = 2$, however, and because of the importance of the surface in carrier dynamics (as outlined in Sec. I) we may interpret the data to support these findings.

At lower temperatures, one expects multiple trapping to give way to either hopping transport or tunneling between localized states. The temperature-independent nature of β as the samples are cooled is consistent with these models. In either case one may extract the dimension d from the observed values of β : in glass *B*, d remains close to 2 (1.7 ± 0.4), while that in glass *A* becomes 1.1 ± 0.1 . An exact explanation of the different behavior between the two glasses would require a microscopic model of the energy surface morphology of each of the nanocrystals. Based on TEM images of the samples, we may speculate that this difference is related to the shape of the crystals. The small crystallites of glass *B* appear spherical, while the larger crystallites of glass *A* appear to have acquired some of the elongated and faceted nature of larger crystals.²⁰ Our data, then, suggest that at low temperatures motion and recombination along edges is preferred over motion across surfaces.

To distinguish between hopping or tunneling transport, both of which predict a temperature-independent β at low temperatures, one may examine the behavior of τ . Tunneling would imply a temperature-independent τ , as thermal effects are not considered in this type of transport. While this regime was observed in a similar experiment performed on C_{60} polycrystalline films,³⁶ Fig. 10 clearly shows that τ depends on temperature in our system. Variable-range-hopping models predict that the

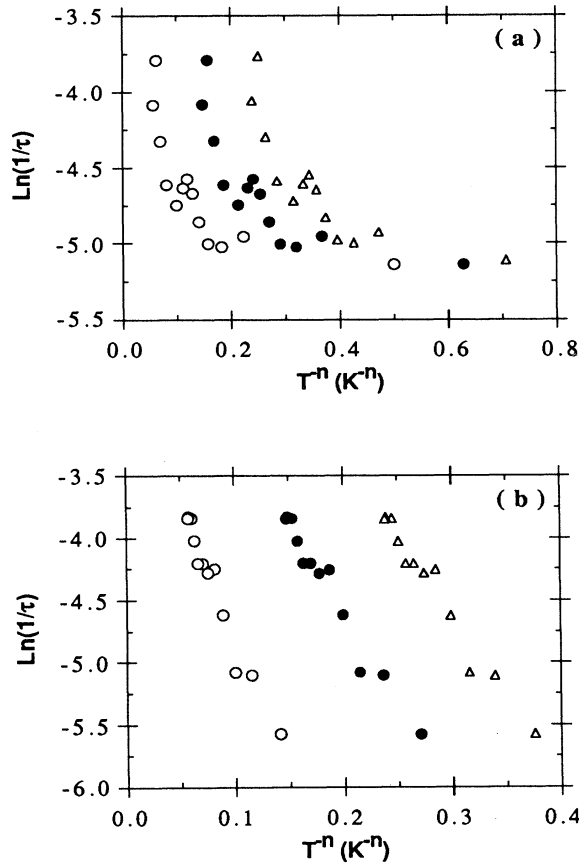


FIG. 10. Low-temperature behavior of τ for glasses *A* and *B* in (a) and (b), respectively. In each graph are plots of $\ln(1/\tau)$ vs $T^{-1/(d+1)}$ for $d=1$ (open circles), $d=2$ (filled circles), and $d=3$ (open triangles), where $1/\tau$ is computed in ps^{-1} and T is given in K before taking the inverse power. A linear curve on any of these axes indicates consistency with activated hopping as described in the text.

mean hopping time τ_0 varies with temperature as³⁷

$$\tau_0^{-1} = \nu_{\text{ph}} \exp\{-BT^{-1/(d+1)}\}, \quad (3)$$

where ν_{ph} is an attempt-to-escape frequency, usually taken as the phonon frequency, and

$$B \propto \left\{ \frac{\alpha^3}{kN(E_F)} \right\}^{1/(d+1)}, \quad (4)$$

where k is the Boltzmann constant, $N(E_F)$ is the density of states at the Fermi level, and α is the decay length of localized-state wave functions. As shown in Fig. 10(b) the variation of τ with T in sample *B* is reasonably well described by the variable-range-hopping model. However, the fit of the data to Eq. (3) is rather insensitive to the value of d in the range $1 < d < 3$: in all cases the plot of $\ln(1/\tau)$ versus $T^{-1/(d+1)}$ gives straight lines. The analysis of the measured variation of τ leads to estimates

only of the model variables ν_{ph} , $N(E_F)$, and α rather than to useful values. This is because τ is not related in a straightforward way to τ_0 . By comparison of our fitting function to Eq. (2) for $d=2$ and $p < 1$, $\tau = \tau_0 C^2 p$. With $C=1$ and p in the range $10^{-1} < p < 10^{-3}$, the extracted value for ν_{ph} is $10^{-10} \text{ s}^{-1} < \nu_{\text{ph}} < 10^{-12} \text{ s}^{-1}$. Assuming that $1/\alpha = 1 \text{ nm}$, we obtain $N(E_F) = 4 \times 10^{21} \text{ cm}^{-3} \text{ eV}^{-1}$. Both are reasonable values, considering that the LO phonon frequencies in CdSe and CdS are from 6×10^{12} to $9 \times 10^{12} \text{ s}^{-1}$ (Ref. 38), and that $N(E_F)$ is of the order of the density of states at the band edge in semiconductors.

The variation of τ with T in sample *A*, however, is not strong enough to be fitted properly to the variable-range-hopping model with $1 < d < 3$. This is rather puzzling, since one would expect two such similar systems to be qualitatively consistent with the same transport models. Further work will have to be done to determine the origin of the temperature dependence of τ in glass *A* at low temperatures.

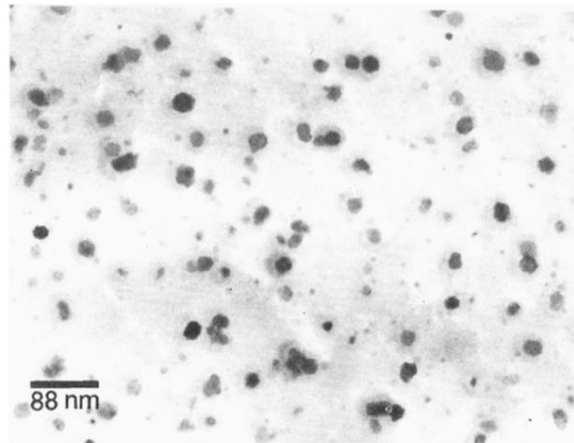
V. CONCLUSIONS

In conclusion, we have examined the picosecond relaxation of photoexcited charge carriers in two $\text{CdS}_x\text{Se}_{1-x}$ nanocrystallite glasses as a function of temperature. A model is proposed in which carriers are quickly localized to surface states and recombine on recombination centers reached via continuous-time random walks. This model predicts stretched exponential decays that are functions of two parameters τ and β . Analysis of $\beta(T)$ reveals that for $300 \text{ K} < T < 450 \text{ K}$ this picture is consistent with carrier transport governed by multiple-trapping processes confined to two dimensions. At temperatures from room temperature down to 4 K, β is independent of T for the larger crystallite glass, glass *A*, and consistent with activated hopping transport further confined to a dimension near 1. This model of transport is supported by the analysis of τ . We speculate that the carriers in this sample may preferentially move along facet edges as opposed to over the surfaces of these larger nanocrystals. The low-temperature variation of β in the smaller crystallite glass, glass *B*, is consistent with dynamics confined to two dimensions, but the observed variation of τ is not consistent with activated hopping.

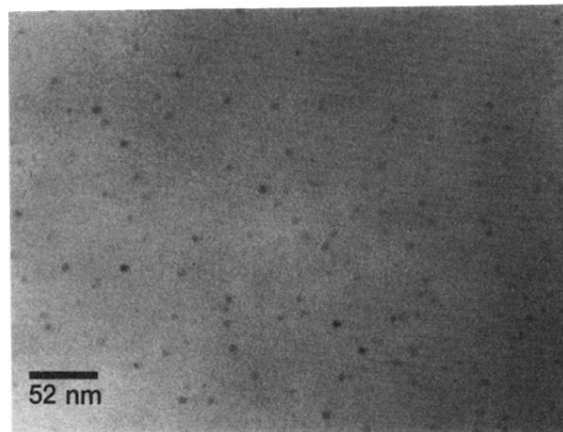
ACKNOWLEDGMENTS

The authors would like to thank J. Tauc and J.C. Phillips for helpful discussions concerning dispersive transport models. G.B. is grateful to the Department of Education and to AASERT for support at various times during this work. E.S. thanks the Swiss National Fund for Scientific Research for their financial support. A.S.L.G. thanks CNPq for his funding. N.M.L. is grateful to the U.S. Air Force Office of Scientific Research for supporting this work.

- ¹R. K. Jain and R. C. Lind, *J. Opt. Soc. Am.* **73**, 647 (1983).
- ²A. L. Éfros and A. L. Éfros, *Fiz. Tekh. Poluprovodn.* **16**, 1209 (1982) [*Sov. Phys. Semicond.* **16**, 772 (1982)].
- ³P. Roussignol, D. Ricard, J. Lukasik, and C. Flytzanis, *J. Opt. Soc. Am. B* **4**, 5 (1987).
- ⁴A. Henglein, *Ber. Bunsenges. Phys. Chem.* **86**, 301 (1982).
- ⁵M. O'Neil, J. Marohn, and G. McLendon, *J. Phys. Chem.* **94**, 4356 (1990).
- ⁶U. Woggon, M. Müller, I. Rückmann, J. Kolenda, and M. Petruskas, *Phys. Status Solidi* **160**, K79 (1990).
- ⁷T. Dannhauser, M. O'Neil, K. Johansson, D. Whitten, and G. McLendon, *J. Phys. Chem.* **90**, 6074 (1986).
- ⁸J. Kolenda, U. Woggon, M. Müller, I. Rückmann, M. Petruskas, and J. Kornack, *Superlatt. Microstruct.* **9**, 331 (1991).
- ⁹Robin R. Chandler, Jerry L. Coffey, Stephen J. Atherton, and Paul T. Snowden, *J. Phys. Chem.* **96**, 2713 (1992).
- ¹⁰Tijana Rajh, Olga I. Micic, Darren Lawless, and Nick Serpone, *J. Phys. Chem.* **96**, 4633 (1992).
- ¹¹Shelli Bingham and Jeffery L. Coffey, *J. Phys. Chem.* **96**, 10581 (1992).
- ¹²S. A. Majetich and A. C. Carter, *J. Phys. Chem.* **97**, 8727 (1993).
- ¹³M. Nirmal, C. B. Murray, D. J. Norris, and M. G. Bawendi, *Z. Phys. D* **26**, 361 (1993).
- ¹⁴Masaharu Mitsunaga, Hiroyuki Shinojima, and Ken-ichi Kubodera, *J. Opt. Soc. Am. B* **5**, 1448 (1988).
- ¹⁵Makoto Tomita, Takahiro Matsumoto, and Masahiro Matsuoka, *J. Opt. Soc. Am. B* **6**, 165 (1989).
- ¹⁶U. Woggon, I. Rückmann, J. Kornack, M. Müller, J. Cesnulevicius, M. Petruskas, and J. Kolenda, *J. Cryst. Growth* **117**, 608 (1992).
- ¹⁷B. Van Wonerghem, S. M. Saitel, T. E. Dutton, and P. M. Rentzepis, *J. Appl. Phys.* **66**, 4935 (1989).
- ¹⁸M. Ghanassi, M. C. Schanne-Klein, F. Hache, A. I. Ekimov, D. Ricard, and C. Flytzanis, *Appl. Phys. Lett.* **62**, 78 (1993).
- ¹⁹Douglas R. James and William R. Ware, *Chem. Phys. Lett.* **120**, 455 (1985).
- ²⁰Mireille Allais and Madeleine Gandais, *Philos. Mag. Lett.* **65**, 243 (1992).
- ²¹C. B. Murray, D. J. Norris, and M. G. Bawendi, *J. Am. Chem. Soc.* **115**, 8706 (1993).
- ²²J. Pankove, *Optical Processes in Semiconductors* (Dover, New York, 1975), Chap. 3, Eq. (3-2).
- ²³N. F. Borrelli, D. W. Hall, H. J. Holland, and D. W. Smith, *J. Appl. Phys.* **61**, 5399 (1987).
- ²⁴I. Broser, R. Broser, and A. Hoffmann, in *Semiconductors. Physics of II-VI and I-VII Compounds, Semimagnetic Semiconductors*, edited by O. Madelung, M. Schultz, and H. Weiss, Landolt-Bornstein, New Series, Group III, Vol. 17, Pt. b (Springer-Verlag, Berlin, 1982), Sec. 3.11.
- ²⁵B. Frick, B. Farago, and D. Richter, *Phys. Rev. Lett.* **64**, 2921 (1990).
- ²⁶Michael R. Shlesinger and Elliott W. Montroll, *Proc. Natl. Acad. Sci.* **81**, 1280 (1984).
- ²⁷Lingrong Chen, J. Tauc, and Z. Vardeny, *Phys. Rev. B* **39**, 5121 (1989).
- ²⁸R. V. Chamberlin, George Mozurkewich, and R. Orbach, *Phys. Rev. Lett.* **52**, 867 (1984).
- ²⁹A. Blumen, J. Klafter, and G. Zumofen, in *Optical Spectroscopy of Glasses*, edited by I. Zschokke (Reidel, Dordrecht, 1986), pp. 199-265.
- ³⁰A. Blumen, J. Klafter, and G. Zumofen, in *Transport and Relaxation in Random Materials*, edited by J. Klafter, R. J. Rubin, and M. F. Shlesinger (World Scientific, Philadelphia, 1986), p. 170, Eq. (16).
- ³¹A. Blumen, J. Klafter, B. S. White, and G. Zumofen, *Phys. Rev. Lett.* **53**, 1301 (1984).
- ³²G. Pfister and H. Scher, *Adv. Phys.* **27**, 747 (1978).
- ³³Edwin F. Hilinski, Patricia A. Lucas, and Ying Wang, *J. Chem. Phys.* **89**, 3435 (1988).
- ³⁴M. G. Bawendi, W. L. Wilson, L. Rothberg, P. J. Carroll, T. M. Jedju, M. L. Steigerwald, and L. E. Brus, *Phys. Rev. Lett.* **65**, 1623 (1990).
- ³⁵S. Juršėnas, M. Strumskis, A. Žukauskas, and A. I. Ekimov, *Solid State Commun.* **87**, 577 (1993).
- ³⁶R. A. Cheville and N. J. Halas, *Phys. Rev. B* **45**, 4548 (1992).
- ³⁷N. F. Mott and E. A. Davis, *Electronic Processes in Non-Crystalline Materials*, 2nd ed. (Clarendon, Oxford, 1979).
- ³⁸I. Broser, R. Broser, M. Rosenzweig, and A. Hoffmann, in *Semiconductors. Physics of II-VI and I-VII Compounds, Semimagnetic Semiconductors* (Ref. 24), Secs. 3.10 and 3.11.



(a)



(b)

FIG. 1. Bright field transmission electron micrograph of glasses *A* and *B* in (a) and (b), respectively. The samples were mechanically thinned and dimpled, then ion milled and carbon coated. The darker spherical dots are the nanocrystallites. The nanocrystallites in glass *A* are observed to possess an elongated and faceted shape.